Review of re-revised paper:

Evaluation of aerosol optical depths and clear-sky radiative fluxes of the CERES Edition 4.1 SYN1deg data product *by D. Fillmore et al.*

Highlights

- needed paper as MATCH aerosol data are an important element CERES products
- now different larger dust sizes are included (good) … but not correct SSAs (bad)

Concerns

- solar flux validation for aerosol cannot be drawn from AOD data alone – aerosol absorption and aerosol size are also important.
- apparent effect of decreasing SSA at increasing coarse dust sizes is ignored → wrong absorption is assumed

General comments

I have now reviewed the paper several times. This time there were no responses to my latest comments … so I just re-read its content. I am delighted that now larger dust size are considered (great), but unfortunately the associated lower SSA (with larger sizes – for the same RFimag) are ignored. This becomes quite apparent from the supplied simulations in Table 6.
I have provided similar simulations, with the associated stronger AAOD (from lower SSA values) at larger sizes and I could demonstrate that for the particular set-up solar losses to the downward surface fluxes are twice as large with a dust size increase by a factor of 4. Thus, with a stronger mineral dust absorption, it is also likely that the' unresolved' issue for dust regions will disappear.

Thus, please redo your dust simulations and re-evaluate the dust area flux comparisons before publication.

Specific comments

37/38 Clarify this sentence: both Merra and Match are assimilations and the MODIS AOD input is the same. If not explain. Or has this to do that Merra allows for washout processes?

39-42 I assume that refers to Match AOD. So, the surface-flux comparison indicates solar attenuation is too small (-> AOD underestimates and/or absorption underestimates

42-45 So the CERES clear-sky reflection needs more reflection of the surface site (-> AOD overestimates and/or absorption underestimates.

… so if we combine the two findings… then the only conclusion is that MATCH aerosol absorption is underestimated (which for dust is likely an underestimation in size)

46/47 leaving issues unexplained (even in the abstract) is discouraging

167 now several dust sizes are allowed (great !!)

174 the SSA (and ASY) varies with large dust size (and even spectrally), update Figure 1 and simulations! For mineral dust re of 1.5, 2.5, 4.0, 6.5 and 10um the mid-visible SSA values are 0.962, 0.931, 0.918, .882 and .840 for the same imaginary part (here 0.0011). In addition, since the dust solar spectral Rfimag are larger towards the UV the SSA value at shorter wavelengths

are even lower (more absorbing)

223 just curious… are the land-sea contrast offsets of northern Africa a MODIS or a modeling problem? (I do not see very strong offsets in MODIS statistics.)

232 Merrra apparently includes other AOD data from other sources (MISR, AERONET), but MODIS data should dominate (in volume) so I would not expect so significant differences as displayed in Figure 3. How can you exclude that model-specific aerosol processing in the base-line model (without assimilations) is not the issue. This could be easily verified … or?

259 the least square fits and rms values (in figure 4) are dominated by the largest AOD, but not by the most frequent AOD, thus possibly also show the scatter plots in log/log scale

459 yes! … and remember a larger coarse dust size can also increase the aerosol absorption

489 this table is interesting and quite revealing. To demonstrate, I did similar simulations, using a solar zenith angle of 0.95 (not 1, oh well but close), a desert surface albedo, a mid-lat summer atmosphere, and dust with (only) a mid-visible optical depth of 0.2 for mineral dust located between 1 and 3 km altitude. Here different dust sizes with their associated SSA are applied (all dust size-distributions assume the same spectral refractive indices with RFimag at 550nm = 0.0011). The downward shortwave and longwave fluxes of these simulations are

		shortwave	longwave
No dust		998	346
Dust (0.2)	reff= 1.5um	985	354
Dust (0.2)	reff= 2.5um	983	357
Dust (0.2)	reff= 4.0um	980	359
Dust (0.2)	reff= 6.5um	974	359
Dust (0.2)	reff= 10.um	968	359

These calculations consider the lower SSA at larger size (as they should) and the solar losses at the surface flux losses for factor 4 dust size increase with these calculations are:
-15 W/m2 (between reff 10 and reff 2.5) while the author's simulations - even with larger u0 (=1) - 8 W/m2 (between reff 8 and reff 2). So please redo your calculations with the correct (lower) ssa values at larger sizes … and you will have an explanation to your dust bias.

And the LW dust impact on downward fluxes depends strongly on the assumed dust vertical distribution as much as on size. Thus, all size (… from AeroNet inversions?), correct RFimag (especially in the stronger absorbing 8-10um region … from I.Sokolik?) and altitude (…from Calipso?) have to all accurate for useful clear-sky dn LW flux comparisons at the surface.

So when the correct dust sizes/SSAs are applied with the result of a stronger aerosol absorption possibly (with the right dust sizes, and right dust altitutes) correction to AOD and water vapor may not be necessary to bring SW and LW fluxes into agreement.

577 more clouds → more AOD? … not for dust, when clouds remove dust

593 redo your large dust SSA calculations … and the solar surface vs toa flux difference problem for mineral dust should be gone.

Below I attach a summary of the top-down (optics → component) approach of the MAC climatology, which lists in Table A1 different dust types, in Figure A3 (column3) seasonal averages of dust size (based on AAODc and AODc-DU), assumed size-distributions and spectral refractive indices in Figure A6 and resulting single scattering properties in Figure A7 (where 'DU+' is for larger dust with reff =4um and 'DU' is for background dust with reff=1.5um).

MAC v3 details

The Max-Planck Aerosol Climatology (MAC) offers merged monthly global maps for aerosol optical properties. In the merging process, multi-annual observational statistics of photometry from the ground is forced on spatial context supplied aerosol component 'bottom-up' modeling. The merged aerosol optical properties focus on aerosol column amount and aerosol column absorption, separately for smaller 'fine-mode' aerosol and larger 'coarse-mode' aerosols. In Figure A1, multi-annual averages from photometry (AERONET/MAN with absorption data only over continents) are compared to multi-(AeroCom phase 3) model interquartile averages (AC3-iqa). In addition, in that Figure A1 the resulting MAC version 3 maps are presented along with applied regional % changes to AC3-iqa.

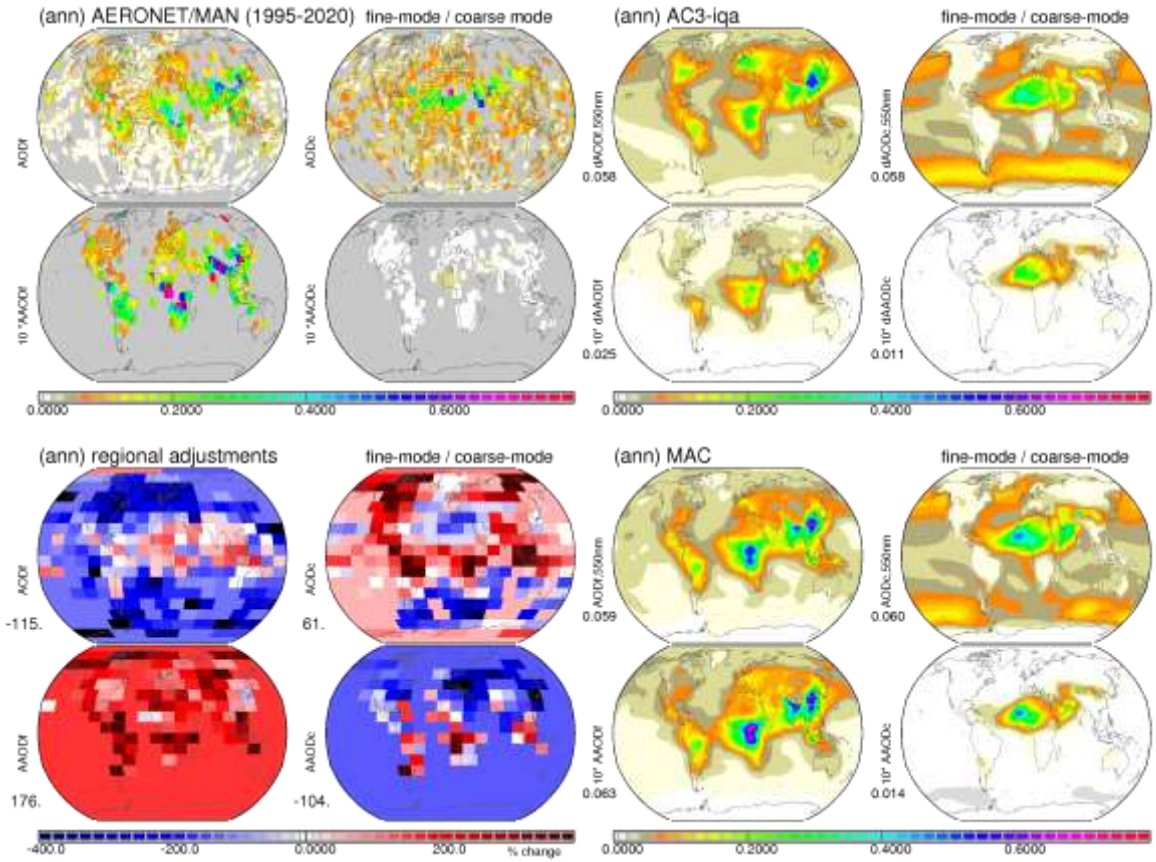

Figure A1. *Global annual average distributions for AODf, AAODf, AODc and AAODc of (1) AERONET/MAN photometry (upper left), (2) the AeroCom phase III multi-model interquartile average background (AC3-iqa, upper right) and (3) resulting MAC climatology fields (lower right) - after AERONET/MAN adjustments in % to AC3-iqa (lower left). Numbers at the lower left of each image indicate global averages. Also note that absolute aerosol absorption data (AAOD) are multiplied by 10 to match the common scale.*

Major adjustments to the 'bottom-up' modeling background are strong increases to the 'fine-mode' absorption (AAODf) and decreases to the 'fine-mode' aerosol amount (AODf) at mid-latitudes. Also SH continental dust (AODc) is stronger. Absolute MAC version 3 changes with respect to both

background (AC3-iqa) and to the older version2 of the MAC climatology (*Kinne, 2019a*) are presented in Figures A2 and A3.

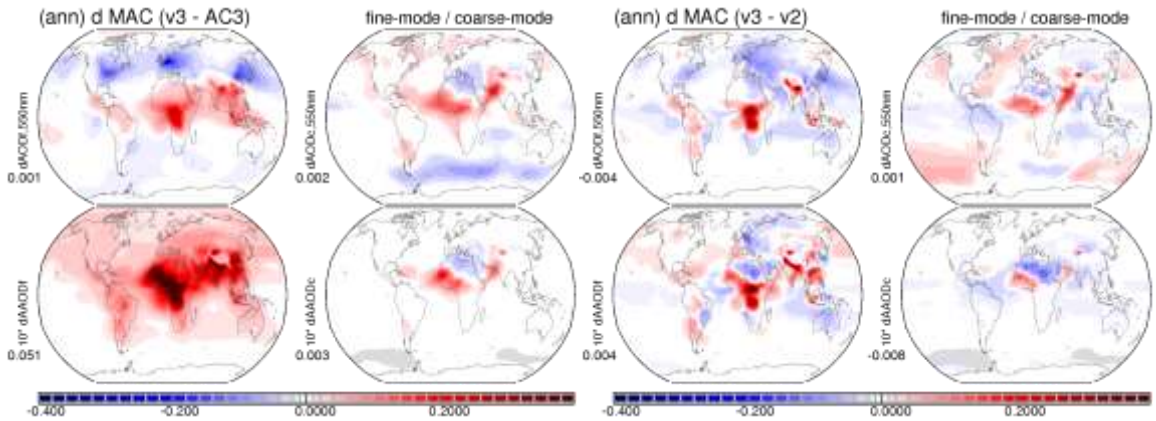

Figure A2. *Absolute annual difference global distributions for AODf, AAODf, AODc and AAODc between the MAC (v3) climatology and the AC3-iqa background (left block) or the older version (v2) of MAC (right block). Average differences are summarized by a value and for the common scale absorption data differences were multiplied by 10.*

Compared to the previous MAC (v2) version (*Kinne 2019a*), the new MAC (v3) climatology version uses and more recent (better emission data applying and component mixture permitting) modeling AC3-iqa background (instead of the AC1-median) and considers 238 (instead of 21) sub-regions for regional adjustments. This resulted in different fine-mode distributions over E. Asia on strongly increased fine-mode contributions over central Africa.

In a 'top-down' approach aerosol column and absorption properties are associated with a mixture of pre-defined aerosol components, that differ in size and mid-visible absorption. All MACv3 types are listed in Table 1.

Table A1. *size and absorption potential of pre-defined aerosol types in MACv3. Listed are (1) effective radii (Re) of log-normal distributions with associated mode radii (Rm) and standard deviations (sd), (2) mid-visible refractive indices (and from size and RF,imag resulting SSA values) and (3) column numbers (N) based on component global mid-visible AOD averages. Five different sizes are allowed for sulfate and dust, each. For comparison, values of a cumulus water cloud (water) and a cirrus cloud (ice) are provided.*

aerosol type	label	Re	Rm	s_d	RF_R	RF_I	SSA	< OD >	N
		[um]	*[um]*		*at 550nm wavelength*				*[#/m2]*
soot (not used)	BC	.06	.03	1.7	1.70	.7000	.155	0.005	4.0 e+11
soot + o.shell	**BO**	**.12**	**.08**	**1.5**			**.615**	**0.015**	**4.0 e+11**
organic	**OC**	**.18**	**.12**	**1.5**	**1.53**	**.0050**	**.975**	**0.022**	**1.8 e+11**
sulfate	SU	.06	.03	1.7	1.43	.0000	.999	0.023	4.4 e+13
sulfate	SU	.10	.05	1.7	1.43	.0000	.999	0.023	4.1 e+12
sulfate	**SU**	**.16**	**.08**	**1.7**	**1.43**	**.0000**	**.999**	**0.023**	**6.0 e+11**
sulfate	SU	.26	.13	1.7	1.43	.0000	.999	0.023	1.2 e+11
sulfate	SU	.40	.20	1.7	1.43	.0000	.999	0.023	3.8 e+10

seasalt	**SS**	**2.5**	**.75**	**2.0**	**1.50**	**.0000**	**.999**	**0.035**	**3.3 e+09**
dust	**DU**	**1.5**	**0.93**	**1.55**	**1.53**	**.0011**	**.962**	**0.025**	**2.7 e+09**
dust	DU	2.5	1.34	1.7	1.53	.0011	.931	0.025	1.3 e+09
dust	DU	4.0	1.55	1.85	1.53	.0011	.918	0.025	7.0 e+08
dust	DU	6.5	1.98	2.00	1.53	.0011	.882	0.025	3.6 e+08
dust	DU	10	2.30	2.15	1.53	.0011	.840	0.025	2.0 e+08
cloud **water**	water	10	6.7	1.5	1.33	.0000	.999	10.0	2.5 e+10
cloud **ice**	Ice	40	20	1.7	1.31	.0000	.999	0.5	1.1 e+08

For smaller fine-mode sizes (1) a strongly absorbing BO (a soot coated by organic material) type, (2) a weakly absorbing organic matter (OC) type and (3) a non-absorbing sulfate (SU) type are considered. Thus, the SU type includes other non-absorbing fine-mode contributions, as from nitrate or seasalt. In order, to separate absorption contributions between BO and OM, the BO/(BO+OM) ratios for AOD from AeroCom 'bottom-up' modeling are applied (i.e. BO/(BO+OM) AOD ratios are higher over urban pollution than over wildfire regions). While BO (Re=0.12um, with Re=0.06um BC cores) and OM (Re=0.18um) sizes are fixed, the SU size (0.06 < Re < 0.40um) remains variable to match fine-mode effective radii of the MAC climatology.

For larger coarse-mode sizes (1) a non-absorbing seasalt (SS) type and (2) an absorbing mineral dust (DU) type, are assumed. While the SS (Re=2.5um) size is fixed, the DU size (1.5 < Re <10um) is assumed to increase with coarse-mode DU-AOD. Note that even with a constant mid-visible imaginary part for dust – here assumed at 0.0011 (*Di Biagio, 2019*) – the mid-visible absorption potential ($1\text{-}SSA_{DU}$) increases with dust size. With an initial guess for the SS-AOD to extract the AODc associated with mineral dust, the following relationship is applied:

$$1\text{-}SSA_{DU} = 1\text{-}SSA_{DU,min} + 0.05 * \text{DU-AOD}$$

$1\text{-}SSA_{DU,min}$ = 0.037 (for the smallest assumed dust aerosol radius of 1.5um)
DU-AOD = (AODc – SS-AOD,guess)
SS-AOD,guess = $.003 * \text{windspeed}_{SUR}$ [m/s] *(2-cos (2* (lat[deg]-sun[deg])/2)
*(ocean_fraction)

As the coarse-mode absorption now defines both the DU-AOD and the size for dust, and the remaining coarse-mode AOD is assigned to seasalt to replace the initial SS-AOD guess.

Figure A3 presents seasonal averages for 'top-down' size-choices for sulfate and dust components, for the fine-mode Re of MAC and for the applied BO/(BO+OM) ratios from modeling.

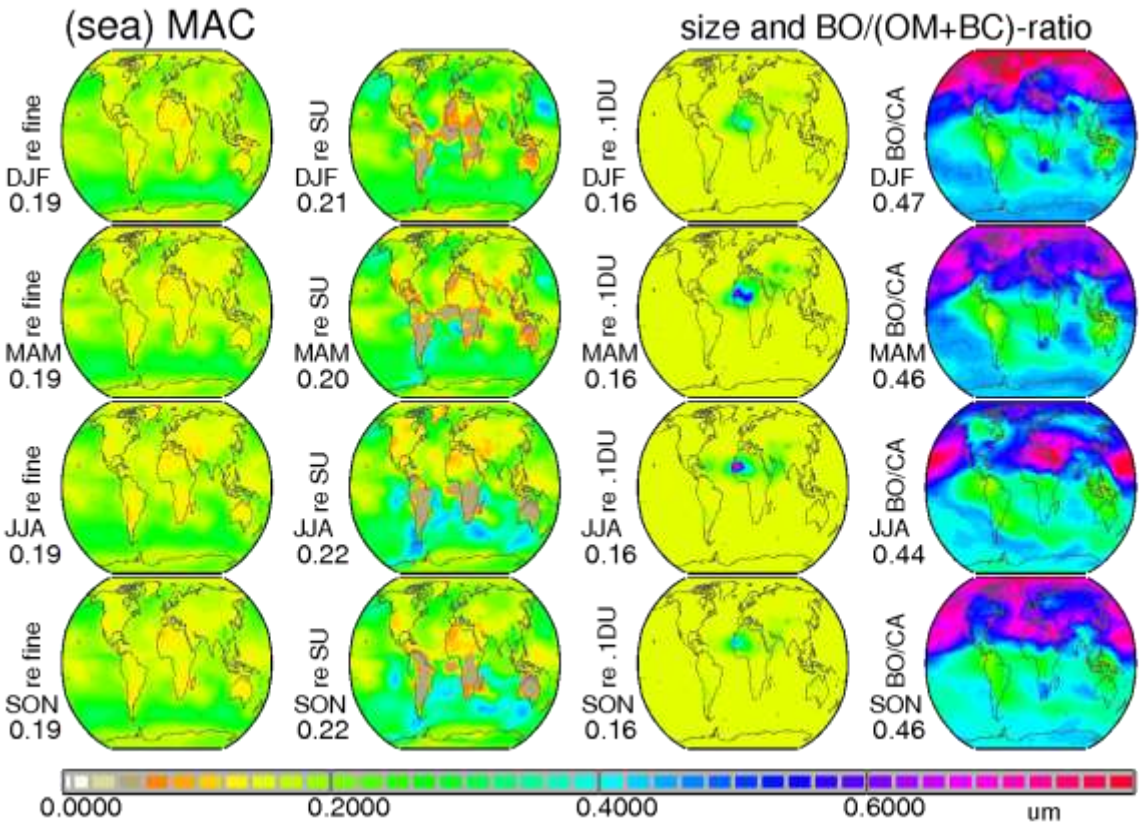

Figure A3. *MACv3 seasonal maps for fine-mode Re (col1) and as part of the 'top-down' approach sizes (Re) for non-absorbing fine-mode (col2) and mineral dust (col3 – times 0.1, to fit common scale). Also presented are applied BO/(BO+OM) ratios from modeling (col4) to separate BO and OM. Numbers next to plots show seasonal averages.*

The resulting aerosol component AOD maps attributed in the 'top-down' approach are presented Figure A4: seasalt (SS) and dust (DU) from AODc and sulfate (SU), organic carbon (OC) and black carbon from AODf.

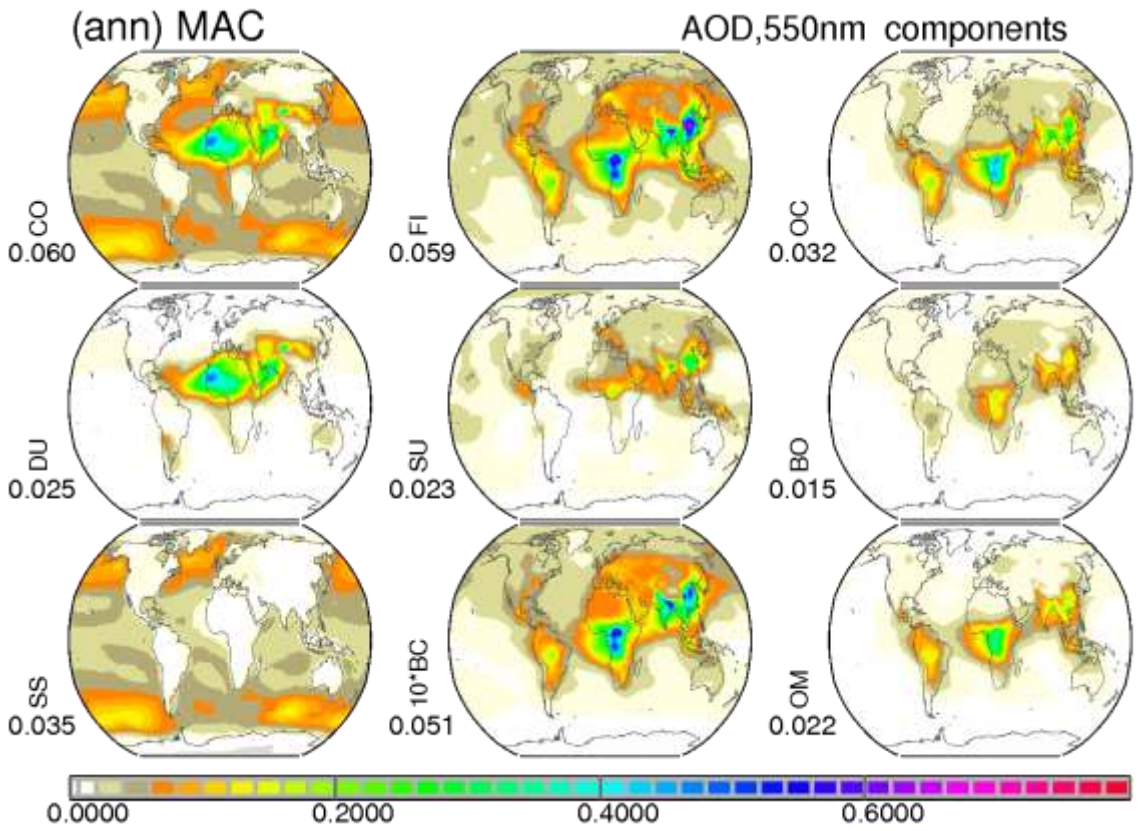

Figure A4. *MACv3 annual maps of 'top-down' derived AOD component distributions. The coarse mode AOD is split between seasalt (SS) and mineral dust (DU) contributions (left column). The fine-mode AOD is separated into non-absorbing sulfate (SU), strongly absorbing BC (multiplied by 10) and weakly absorbing OC. In a different split for total carbon (CA =OC+BC) contributions without soot (OM) and contributions containing a soot core (BO) are separated. Values next to the maps indicate global averages.*

The annual maps of Figure A4 are a subset of maps shown in Figure 2. To illustrate MAC updates with this version 3 annual difference maps to the previous version 2 (Kinne, 2019a) maps are presented in Figure A5. Global coarse-mode AOD contributions remained stable but DU-AOD is smaller (as well as maximum DU sizes) and SS-AOD is larger. Reduced global fine-mode AOD contributions are caused by significant SU-AOD reductions despite increases to OC-AOD and BC-AOD. Major regional component AOD differences between v 3 and v 2 of MAC are:

DU	- 0.005	more DU over Arab waters, W. Africa, Patagonia, less DU over N. S. Am. and N. Africa
SS	+0.007	more SS over mid-latitude oceans
SU	- 0.015	more SU over N. India and central Africa, less SU over E. Asia, E. Europe, E. US, tropics
OC	+0.010	more OC over central Africa, N. India, SE. Asia, S. America
BC	+0.001	more BC over central Africa, N. India, northern hemisphere

As the fine-mode AOD is smaller, also the anthropogenic (fine-mode) AOD is smaller and less absorbing with the sharp reduction to (scattering) SU-AOD. Also, the anthropogenic (coarse-mode) dust AOD is smaller.

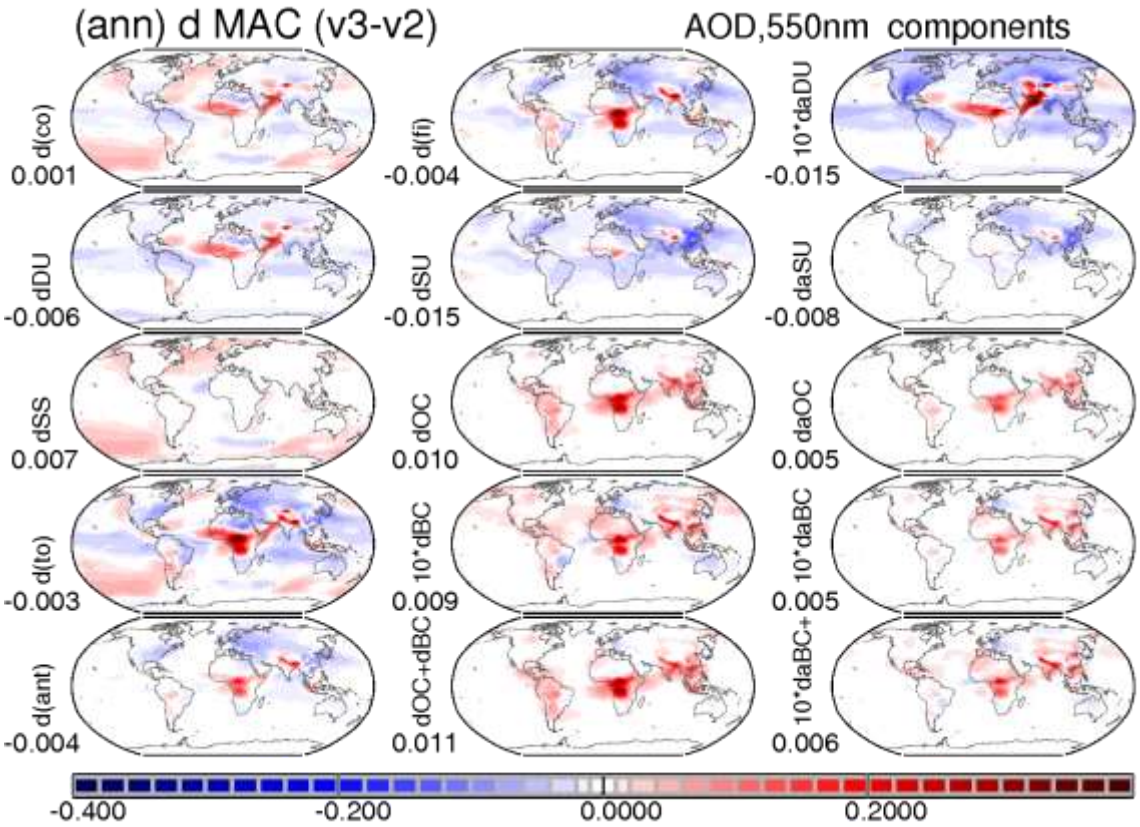

Figure A5. *Absolute annual differences for 'top-down' component AOD data between the current MAC version3 (see Figure 2) and the previous version 2. Values next to the plots indicate global average differences.*

The big advantage of separating AODc and AODf in aerosol components which are completely defined by size (-distribution), composition (with its known refractive indices over the entire spectral solar and infrared spectral region) and shape (here spheres are assumed) is, that all three spectrally varying single scattering properties (as input for broadband radiative transfer simulations) are quickly calculated. This is done via (MIE-) scattering simulations for (1) extinction (EXT, attenuation per distance), (2) single scattering albedo (SSA, the scattering potential) and (3) asymmetry-factor (ASY, approximating the scattering distribution). These single scattering simulations can be done for every desired spectral (radiative transfer) model resolution, as long as the component refractive indices at that resolution are provided. The presented spectral (8 solar and 12 infrared) choices in Figures A6 and A7 below refer to the spectral resolution of the a subsequently used radiative transfer model. The addressed aerosol components in Figure A6 and A7, which were already introduced in Table 1, are soot (BC, Re=0.06um), an organic mixture with a soot core (BO, Re=0.12um), organic material (OC, Re=0.18um), sulfate (SU, Re=0.16um), seasalt (SS, Re=2.5um) and mineral dust (DU, Re=1.5). In addition, properties of a larger mineral dust size (DU+, Re=6.5um) and for a general comparisons also properties for a water cloud (water, Re=10um) and for an ice-cloud (ice, Re=40um) are included. In Figure A6, size-distributions and component refractive indices

are compared. Note, that for the component shell/core mixture of the BO component no combined refractive index is offered (internally calculated) and that for mineral dust and sulfate, independent of a selected aerosol size, the same refractive indices apply.

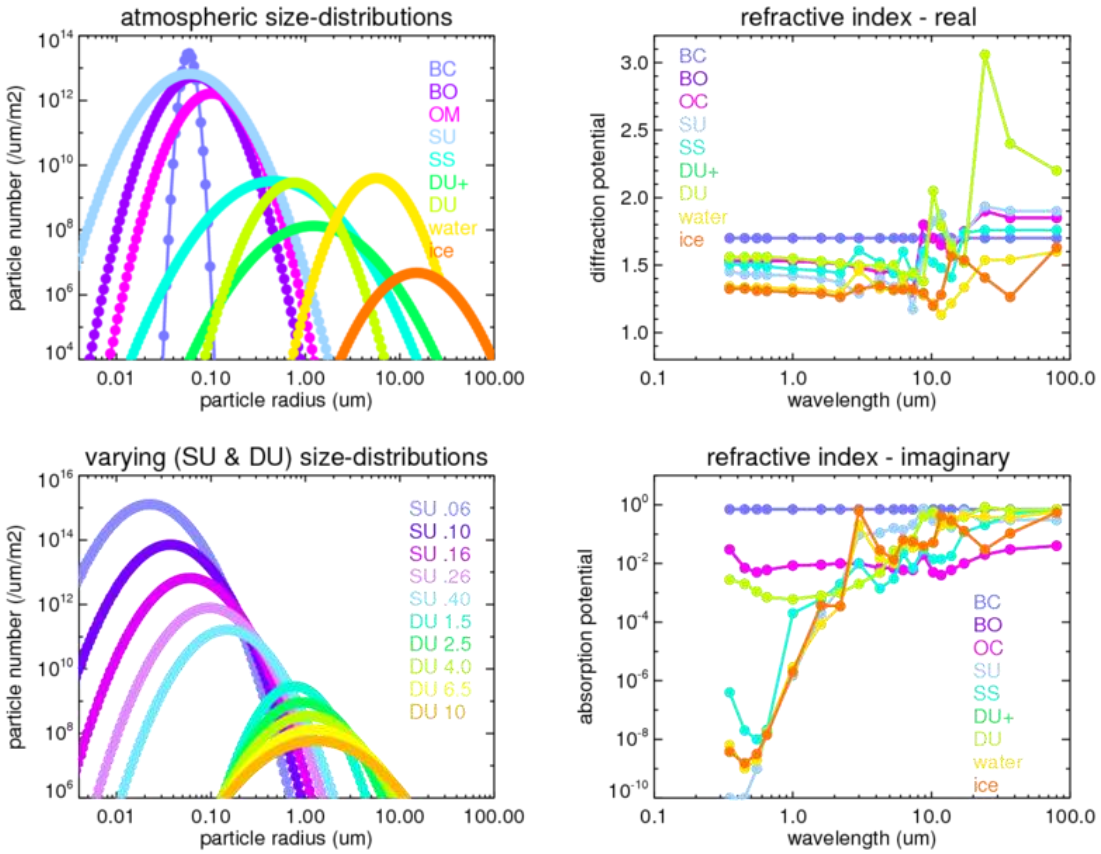

Figure A6. *Aerosol size distributions (left images) for pre-defined aerosol components (to match in presented concentrations the global average MACv3 AOD) and real and imaginary parts of the refractive indices (right images). Refractive indices are compared at central wavelengths of 8 solar and 12 infrared spectral bands. For comparisons, the size distribution and refractive indices for a cumulus cloud and for a cirrostratus cloud are shown.*

Mie simulation (assuming spherical aerosol shapes) then yield the single scattering properties (EXT, SSA, ASY), which are presented for the components of Figure A6 in Figure A7.

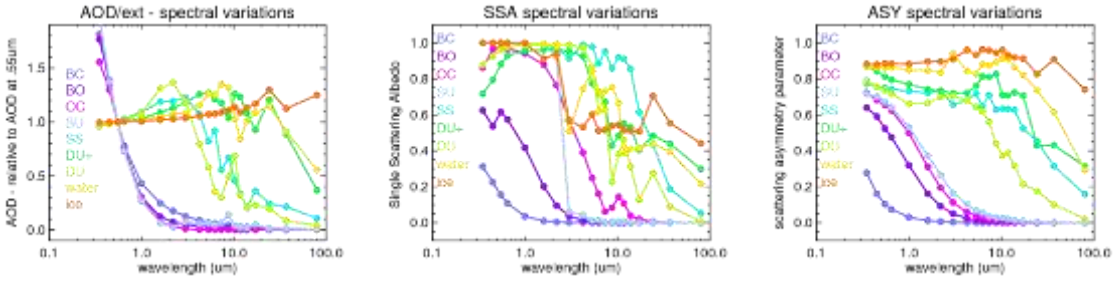

Figure A7. *Calculated spectrally varying component single scattering properties for extinction (left - via the ratios to the component extinction at 550nm), for single scattering albedo (center) and for the asymmetry factor (right).*

According to AOD maps of Figure A4, component single scattering properties are combined (AOD is additive, SSA is weighted by AOD and ASY is weighted by AOD*SSA) to yield global maps. Resulting single scattering properties at four selected wavelengths for fine-mode and coarse mode aerosol are presented in Figure A8.

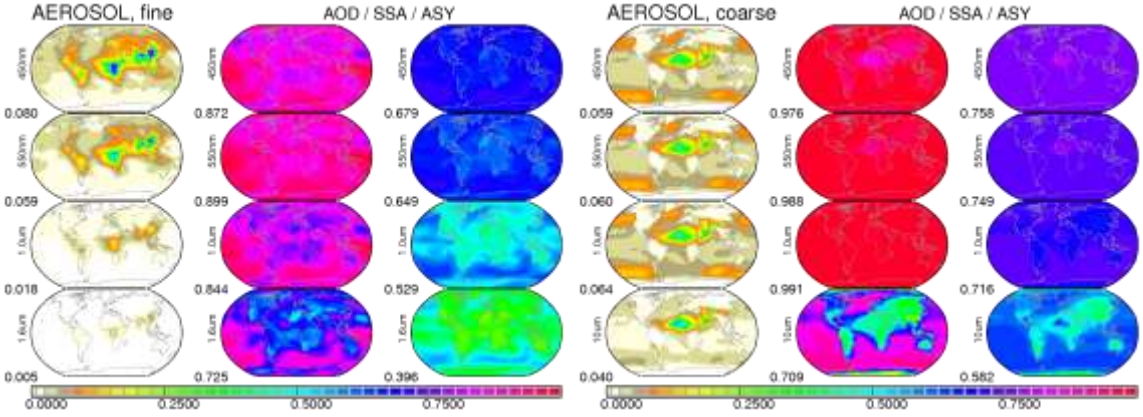

Figure A8. *Component combined annual average single scattering properties maps (AOD – left col., SSA – center col., ASY – right col.) at four selected wavelengths: at .45, .55, 1.0 and 1.6um for the fine-mode AOD (left) and at .45, .55, 1um and 10um for the coarse-mode AOD (right). Numbers at the lower left indicate global annual averages.*

Note that for the fine-mode, the aerosol sizes are too small to yield significant radiative infrared effects (at wavelengths >4um), so that data are presented at another near-IR wavelength (1.6um - rather than 10um). Similarly to Figure A8, the resulting single scattering properties at four selected wavelengths for (fine-mode) anthropogenic aerosol and for total (fine-mode and coarse-mode combined) aerosol are presented in Figure A9.

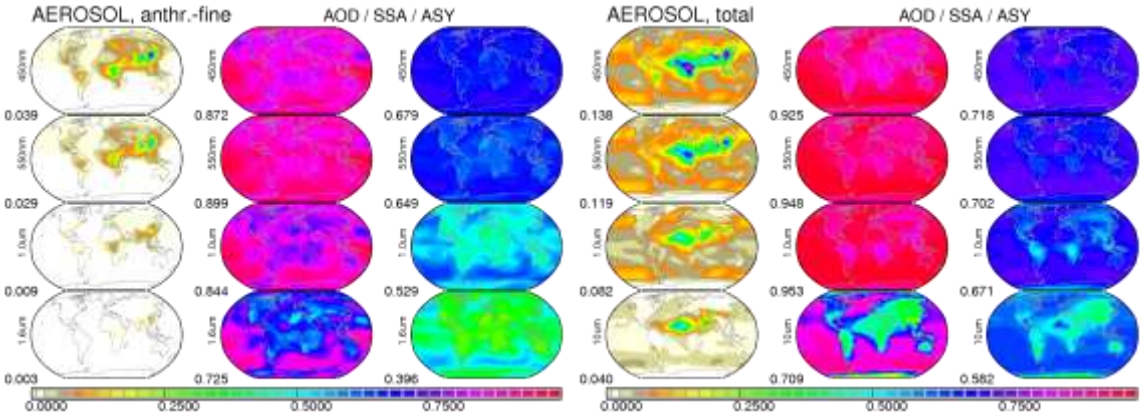

Figure A9. *Component combined annual average single scattering properties maps (AOD – left col., SSA – center col., ASY – right col.) at four selected wavelengths: at .45, .55, 1.0 and 1.6um for anthropogenic*

(fine-mode) AOD (left) and at .45, .55, 1um and 10um for the total AOD (right). Lower left numbers indicate global annual averages.

Now all aerosol needed optical properties are defined, so that radiative transfer simulation can be performed to determine the aerosol radiative effects.